Turkish Journal of Electrical Engineering & Computer Sciences

http://journals.tubitak.gov.tr/elektrik/

Research Article

Turk J Elec Eng & Comp Sci
(2015) 23: 974 – 986
© TÜBİTAK
doi:10.3906/elk-1305-214

A performance comparison of conventional and transverse flux linear switched reluctance motors

Nurettin ÜSTKOYUNCU[1,*], **Krishnan RAMU**[2]

[1]Department of Electrical & Electronics Engineering, Faculty of Engineering, Erciyes University, Kayseri, Turkey
[2]The Bradley Department of Electrical & Computer Engineering, Virginia Tech, Blacksburg, VA, USA

Received: 26.05.2013 • **Accepted/Published Online:** 26.06.2013 • **Printed:** 10.06.2015

Abstract: This paper presents a comprehensive comparison between conventional (longitudinal flux) linear switched reluctance machines (CLSRMs) and transverse flux linear switched reluctance machines (TLSRMs) so as to enable engineers to choose a structure suitable for their applications. A commonly-used single-sided CLSRM and 4 different TLSRM structures are considered for the comparison. For a fair comparison of the 2 types of LSRMs, equal dimensions, including equal length and magnetomotive force, are applied as much as possible. The analytical approach and 3-dimensional finite element analysis (FEA) are employed to obtain the performance of these machines. It is proven analytically that the CLSRM has a higher force capability compared to TLSRMs by as much as 6 times under linear B-H characteristic operating points. The results are reinforced by the FEA-based performance results. Furthermore, the CLSRMs are simpler to construct, resulting in lower manufacturing cost and thus paving an easier path for their market acceptance than TLSRMs. These results make CLSRMs the structure of choice for linear-switched reluctance motors.

Key words: Linear switched reluctance motor, transverse flux motor, force density

1. Introduction

Linear switched reluctance machines (LSRMs) are candidates for application consideration owing to their low manufacturing cost (winding only on one side while the other side has nothing but iron), a high fault tolerance, and the availability of numerous low-cost converter topologies to drive them, as compared to other linear electrical machine structures and control techniques that can deliver high performance [1–8].

The LSRM structures are classified into 2 types, known as longitudinal and transverse flux distributed structures, based on the flux direction with respect to the translator's displacement direction. The longitudinal LSRM has a flux direction in the direction of the translator displacement direction, i.e. longitudinally, and is referred to hereafter as a conventional linear switched reluctance machine (CLSRM). The flux lines are perpendicular to the translator displacement direction in transverse flux linear switched reluctance machines (TLSRMs). Recently, some new LSRM structures with transverse flux distribution have been studied to obtain higher force and power densities, as well as higher efficiency [9,10]. TLSRM structures are promoted on the basis of having an inexpensive manufacturing process, a simplified design compared to CLSRM structures, and reported high force density per volume and high efficiency. However, in the literature, there is no detailed comparison between TLSRMs and CLSRMs with longitudinal flux distribution to prove these claims. This paper aims to present research results on the comparison of various types of TLSRMs to a CLSRM and to examine their relative performance.

*Correspondence: nurettinu@erciyes.edu.tr

The analysis of the CLSRM and TLSRM structures are based on performance equations derived from first principles and verified with 3-dimensional finite element analysis (FEA). FEA provides a very accurate performance prediction and a more detailed analysis of the LSRMs. Although 2-dimensional FEA is sufficient for the analysis of CLSRMs, various TLSRM structures, due to their axial dominance, require 3-dimensional FEA. Therefore, for consistency in this study, both CLSRM and TLSRM structures are analyzed using 3-dimensional FEA.

This paper aims to give a comprehensive comparison of the CLSRM and TLSRM structures and is organized as follows. Descriptions of various TLSRM and single-sided CLSRM structures are given in Section 2, preliminary analyses and derivation of the performance equations of the machines are presented in Section 3, and Section 4 covers the results of the comparison and differences in the construction complexities of the machines. Conclusions are summarized in Section 5.

2. Machine structures

A single-sided CLSRM and 4 TLSRM structures are considered, and their dimensions and descriptions are given in this section. The machine structures have equal air gap, stack length, pole length, and stator and translator pole widths. Based on such specifications, the stator and translator volumes, stator, and translator weights are computed for various structures and given in Table 1.

Table 1. Machine dimensions.

Features	Type of LSRMs				
	CLSRM	Type TLSRM	Type 2 TLSRM	Type 3 TLSRM	Type 4 TLSRM
Stator volume (m^3)	4.62e-4	2.38e-4	2.38e-4	1.90e-4	1.90e-4
Translator volume (m^3)	3.53e-4	1.23e-4	0.77e-4	0.84e-5	0.38e-4
Stator weight (kg)	4.14	2.13	2.13	1.70	1.70
Translator weight (kg)	3.16	1.10	0.69	0.76	0.34
Air gap (mm)	1	1	1	1	1
Stator pole width (mm)	20	20	20	20	20
Translator pole width (mm)	24	24	24	24	24
Stack length (mm)	50	50	50	50	50
Stator pole height (mm)	37	37	37	37	37
Stator yoke thickness (mm)	20	16	16	8	8
Translator pole height (mm)	15	15	16	15	8
Translator yoke thickness (mm)	24	16	–	8	–

2.1. TLSRM structures

Four different transverse flux electric machine structures in LSRMs are briefly described below.

2.1.1. Type 1 TLSRM

The type 1 TLSRM consists of a C-core stator and translator, and the stator winding is individual for each pole and placed on the back iron of the stator C-core, as shown in Figure 1a. However, the short depth of the slot limits the number of turns that can be placed and also makes the hand insertion of the preformed windings very difficult in this arrangement. These challenges can be overcome with double windings on the two legs of the C-core as shown in Figure 1b in order to accommodate a higher number of turns as well as the assembly operation with hand insertion of the windings on the limbs.

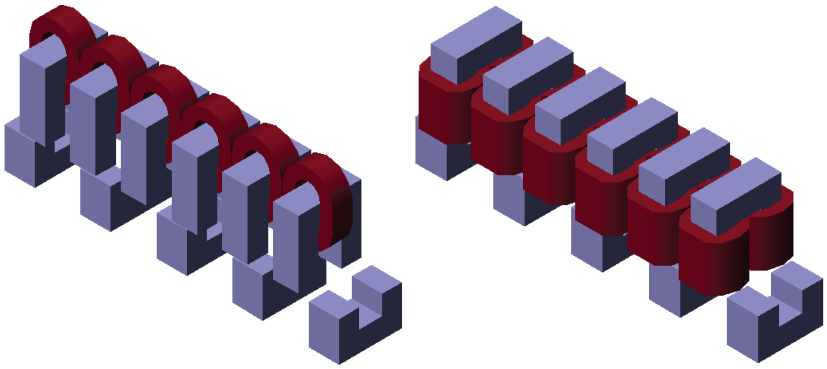

a) b)

Figure 1. Type 1 TLSRM structure.

2.1.2. Type 2 TLSRM

The type 2 TLSRM is very similar to the type 1 TLSRM, except that the translator has I-cores in the place of C-cores as shown in Figure 2a. The same comments on the windings mentioned above for the type 1 TLSRM are also valid for this machine structure. Therefore, double windings should be used as shown in Figure 2b.

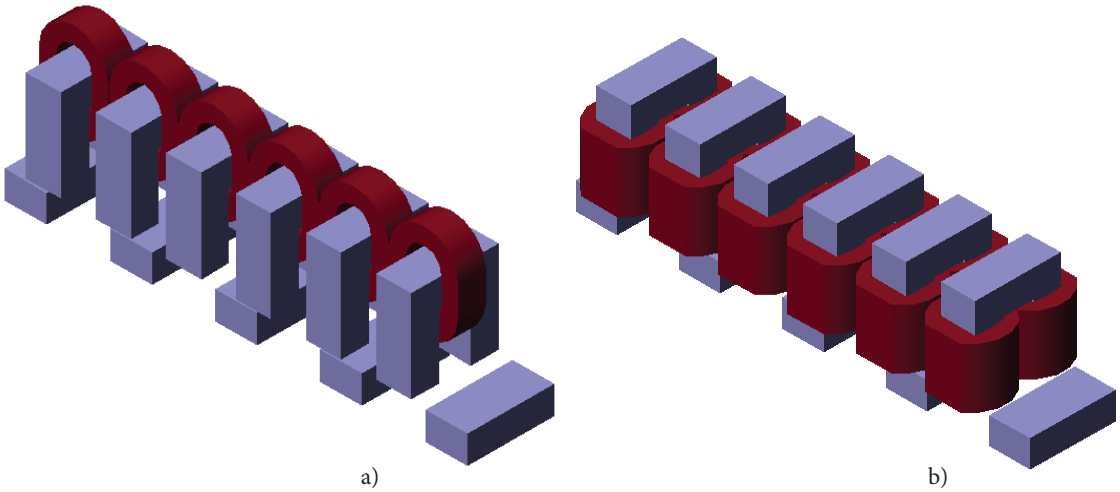

a) b)

Figure 2. Type 2 TLSRM structure.

2.1.3. Type 3 TLSRM

The type 3 TLSRM has the same structure as the type 1 TLSRM except that it has E-cores instead of C-cores both in its stator and translator, shown in Figure 3. The stator winding is placed in the middle limb of the E-core. Note that the mechanical assembly of type 3 remains at the same complexity level of types 1 and 2 TLSRMs.

2.1.4. Type 4 TLSRM

This TLSRM type is very much similar to the type 2 TLSRM except that it has E-cores in place of C-cores in the stator, as shown in Figure 4.

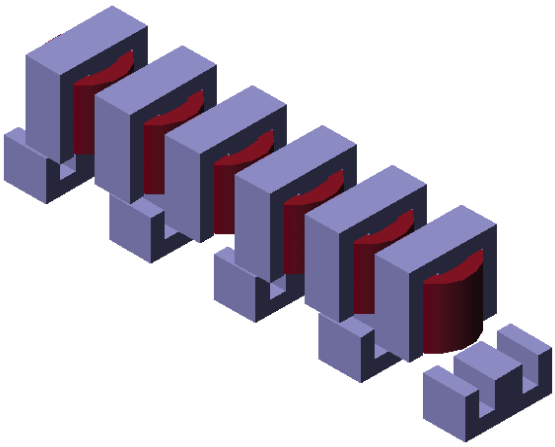

Figure 3. Type 3 TLSRM structure.

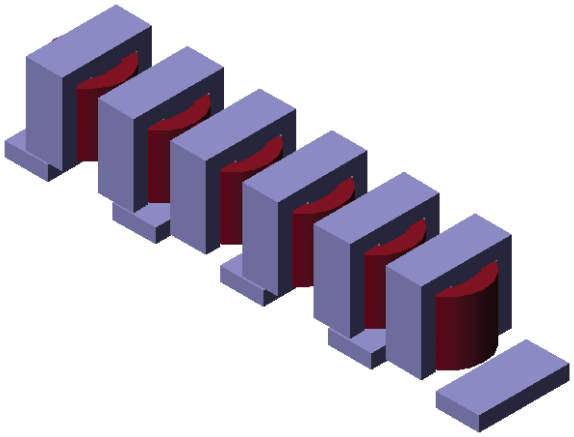

Figure 4. Type 4 TLSRM structure.

2.2. CLSRM structure

A single-sided longitudinal flux electric machine structure in the LSRM has been chosen for comparison with TLSRMs and is described here. This LSRM consists of an opposing stator and translator, as shown in Figure 5.

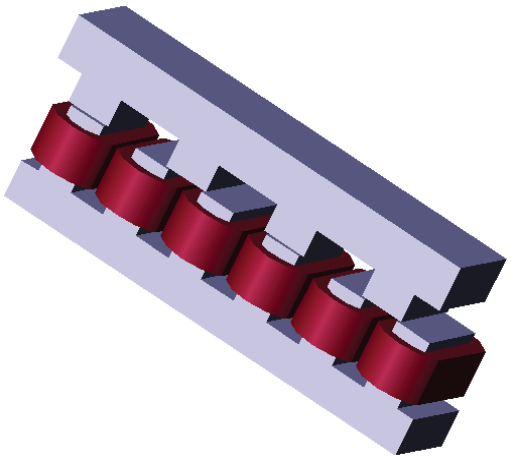

Figure 5. The single-sided CLSRM structure.

An attractive normal force between the stator and translator is generated in this single longitudinal air gap structure, which requires a means of restriction to prevent their coming together. A double-sided structure with two translators and one stator between them balances out the normal forces on the stator [8].

3. Preliminary analysis

The relevant performance equations are derived and presented in this section for a single-sided CLSRM and type 1 and type 2 TLSRMs with similar specifications. The derivations give a clear understanding of the relative force-generating capability of these structures. Considering the linear working region in the machine,

the electromagnetic propulsion force F_{eX} can be written in terms of coenergy as follows:

$$F_{eX} = \frac{dW^{'}}{dx}, \tag{1}$$

where x is the translator position. Coenergy W' in terms of flux linkages λ and current i is given by:

$$W^{'} = \int_{0}^{i} \lambda\left(i,x\right) di, \tag{2}$$

where the flux linkage in terms of the inductance and current is given by:

$$\lambda\left(i,x\right) = L\left(i,x\right)\, i, \tag{3}$$

where L is the inductance of the phase that is a function of the current and translator position. Unaligned inductance and its flux linkages are ignored to achieve a preliminary but conceptual understanding here. Aligned inductance per pole, L_{ap}, can be written in terms of motor dimensions and winding turns as follows:

$$L_{ap} = \frac{N^2}{\Re} = \frac{P_s}{q}\left\{\frac{N^2}{\left(l_g/A\mu_0\right)}\right\}, \tag{4}$$

where P_s is the number of stator poles, N is the number of turns per pole, l_g is the air gap, A is the area of the cross-section of the stator pole at the air gap, μ_0 is the permeability of air, $\Re$ is the reluctance of the magnetic flux path, and q is the phase number. The aligned inductance per phase, assuming 2 poles per phase winding, is given by 2 times the aligned inductance per pole, i.e. $2L_{ap}$. Combining Eqs. (1) through (4) yields the electromagnetic propulsion force in terms of the machine parameters as follows:

$$F_{eX} = 2\left(\frac{\mu_0 P_s A}{2q l_g}\right)\frac{\left(N^2 i^2\right)}{dx}, \tag{5}$$

where dx is the difference between aligned and unaligned translator positions. This equation is used to derive the comparative relationship between CLSRM and TLSRM electromagnetic propulsion forces, represented as F_{eXc} and F_{eXt}, respectively:

$$\frac{F_{eXc}}{F_{eXt}} = \frac{A_c P_{sc} N_c^2}{{}^1\!/_2\, A_t P_{st} N_t^2}, \tag{6}$$

where subscripts c and t represent their respective variables for conventional and transverse flux LSRMs. Here it has been assumed that for both types of LSRM, currents and air gaps are all equal. These are reasonable assumptions for equal power converter requirements for both motors and for equal manufacturing constraints, at least in terms of the air gap. Eq. (7) shows the difference in terms of force generation capability between these structures for the same current and number of turns.

$$\frac{F_{eXc}}{F_{eXt}} = \frac{A_c P_{sc} N_c^2}{{}^1\!/_2\, A_t P_{st} N_t^2} = \frac{3A_t}{{}^1\!/_2\, A_t} \cong 6 \tag{7}$$

The analytical result given in Eq. (7) shows that the electromagnetic force of the CLSRM is almost 6 times that of types 1 and 2 TLSRMs. Note that this is only conceptual, as linear operating conditions are assumed. Whether or not such a difference between their performances does in fact exist will be evaluated by FEA, which will be considered in the following section.

4. FEA-based performance analysis and results

Various design scenarios are considered in this study, such as an equal number of turns per pole in all designs with equal excitation current, equal or similar pole flux densities, and unequal flux densities with equivalent propulsion force. They are simulated for CLSRM and TLSRM designs and the results are presented in this section, along with observations on their constructional complexities. Simulations in the paper are realized using Maxwell 3D software and tetrahedral elements used for mesh operations of motor structures.

4.1. Equal number of turns per pole designs

The force and stator pole average magnetic flux density profiles obtained using FEA of all motor structures for the same number of turns per pole and current are shown in Figures 6 and 7, respectively. Note that types 3 and 4 TLSRM results are plotted for both the average flux density on the central limb as well as the average flux density on the side limbs in Figure 7.

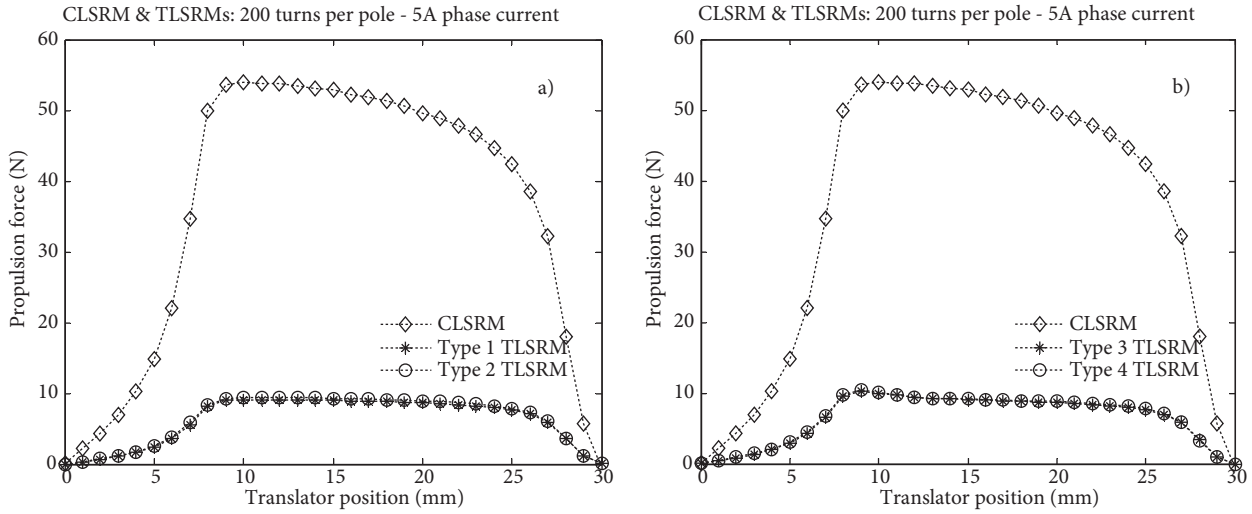

Figure 6. Propulsion forces versus translator position for various types of LSRMs for the same number of turns per pole: a) CLSRM, type 1 and type 2 TLSRMs; b) CLSRM, type 3 and type 4 TLSRMs.

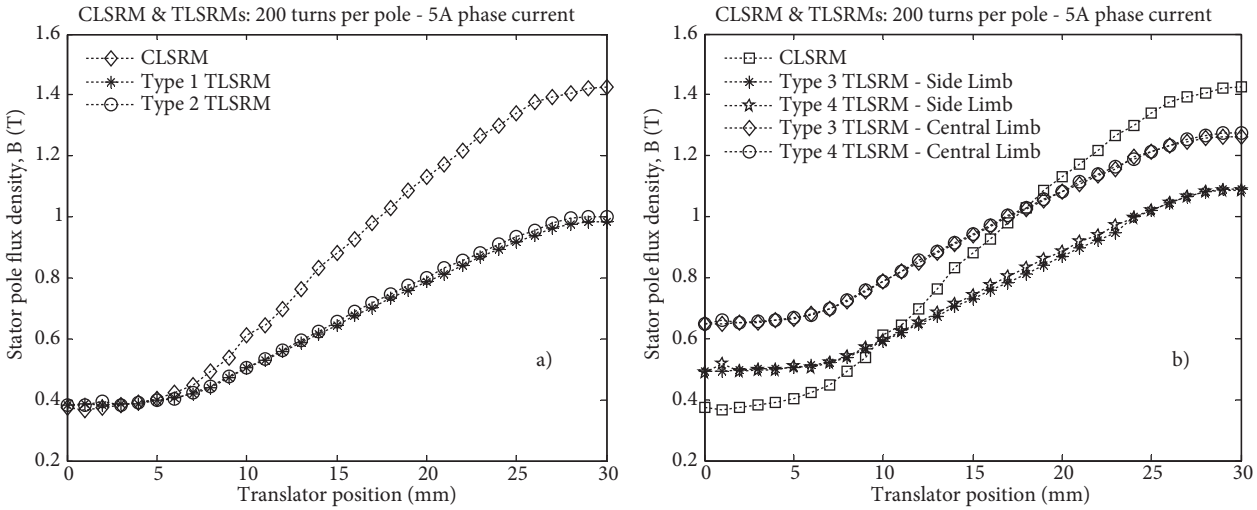

Figure 7. Stator pole flux density versus translator position for various types of LSRMs for the same number of turns: a) CLSRM, type 1 and type 2 TLSRMs; b) CLSRM, type 3 and type 4 TLSRMs.

As shown in Figure 7, FEA analysis proves that the analytical results obtained for the same number of turns and the propulsion force of the CLSRM are almost 6 times those of the TLSRM structures. Some comparisons in terms of the force and force density of the motors for the same magnetomotive force (mmf) excitation are given in Table 2. The force density and average force values of the CLSRM are higher than those of the TLSRM structures for the same number of turns per pole. The CLSRM also does very well by industrial measures such as force density per active motor weight and force density per copper weight. All the simulated force results correspond to ideal current waveforms with turn-on and turn-off instances of 7 and 27 mm, respectively, for the machines under consideration.

Table 2. Comparison of LSRM structures for the same number of turns.

Features	Type of LSRMs				
	CLSRM	Type 1 TLSRM	Type 2 TLSRM	Type 3 TLSRM	Type 4 TLSRM
Number of turns per pole	200	200	200	200	200
Phase current (A)	5	5	5	5	5
Stator volume (m^3)	4.62e-4	2.38e-4	2.38e-4	1.90e-4	1.90e-4
Translator volume (m^3)	3.53e-4	1.23e-4	0.77e-4	0.84e-5	0.38e-4
Winding volume (m^3)	1.86e-4	1.10e-4	1.10e-4	1.07e-4	1.07e-4
Active motor volume (m^3)	10.01e-4	4.71e-4	4.25e-4	3.81e-4	3.35e-4
Stator weight (kg)	4.14	2.13	2.13	1.70	1.70
Translator weight (kg)	3.16	1.10	0.69	0.76	0.34
Winding weight (kg)	1.68	0.98	0.98	0.96	0.96
Active motor weight (kg)	8.98	4.21	3.80	3.42	3.00
Average propulsion force (N)	49.72	8.43	8.71	8.74	8.85
Percentage force (%)	100	16.95	17.52	17.58	17.80
Percentage winding loss (%)	100	58.33	58.33	57.14	57.14
Force density per active motor weight (Nm/kg)	5.54	2.00	2.29	2.55	2.95
Force density per copper weight (Nm/kg)	29.60	8.60	8.89	9.10	9.22

4.2. Equal peak stator pole flux density designs

The required number of turns per pole to achieve the same flux density as that of the CLSRM is found analytically to be 400 for types 1 and 2 TLSRMs. The number of turns per pole of the CLSRM has been fixed at 200 because of the saturation limit of the core and the slot volume limitations of all the machines. The force and stator pole mean flux density profiles of the motors for the selected stator winding turn numbers are shown in Figures 8 and 9, respectively.

Although the stator pole average flux density profiles of TLSRMs are higher than those of the CLSRM, the propulsion force of the CLSRM is higher and almost two times greater than that of TLSRMs with similar specifications, as shown in Figures 8 and 9. The average forces of the motors are compared in Table 3.

Although the average propulsion force of the CLSRM is higher, the force densities per active motor weight of almost all TLSRMs are higher than those of the CLSRM, as given in Table 3. However, it should be noted that all TLSRMs need some special holder structures for separate stator and translator parts. Therefore, the weight and volume of the TLSRM structures will increase when such support structures are included, and then the force density of the motors will decrease, which results in the CLSRM coming out better in the comparisons in this index. In addition, in another useful index, the force density per copper weight of the CLSRM is twice that of the TLSRM structures, thereby proving the superiority of the CLSRM structure over the TLSRM structure.

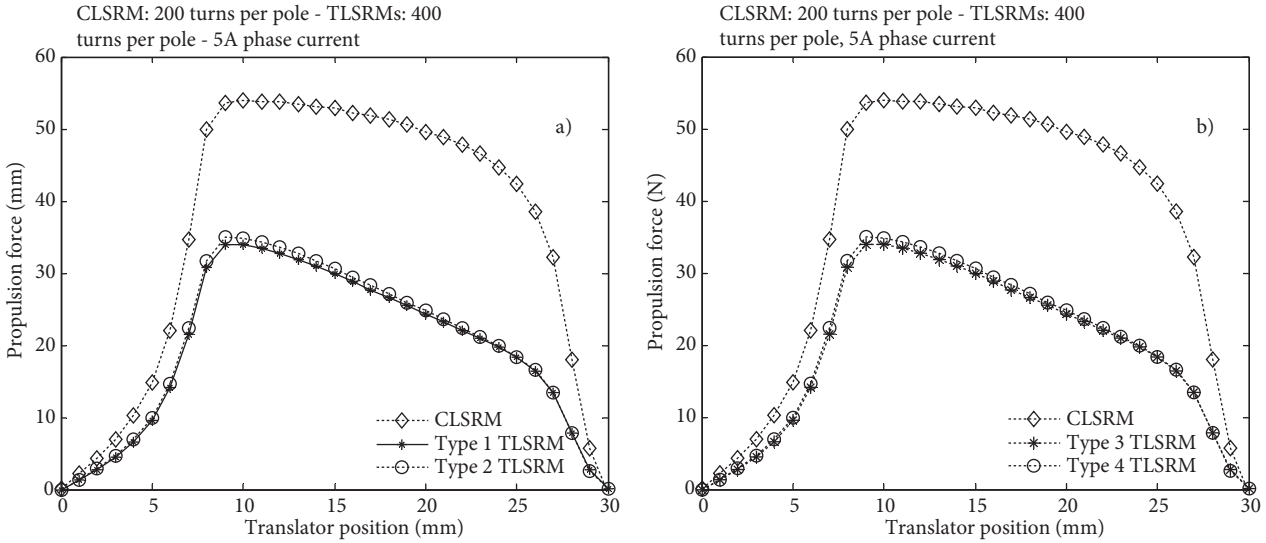

Figure 8. Propulsion forces versus translator position for various types of LSRMs with similar flux density profiles: a) CLSRM, type 1 and type 2 TLSRMs; b) CLSRM, type 3 and type 4 TLSRMs.

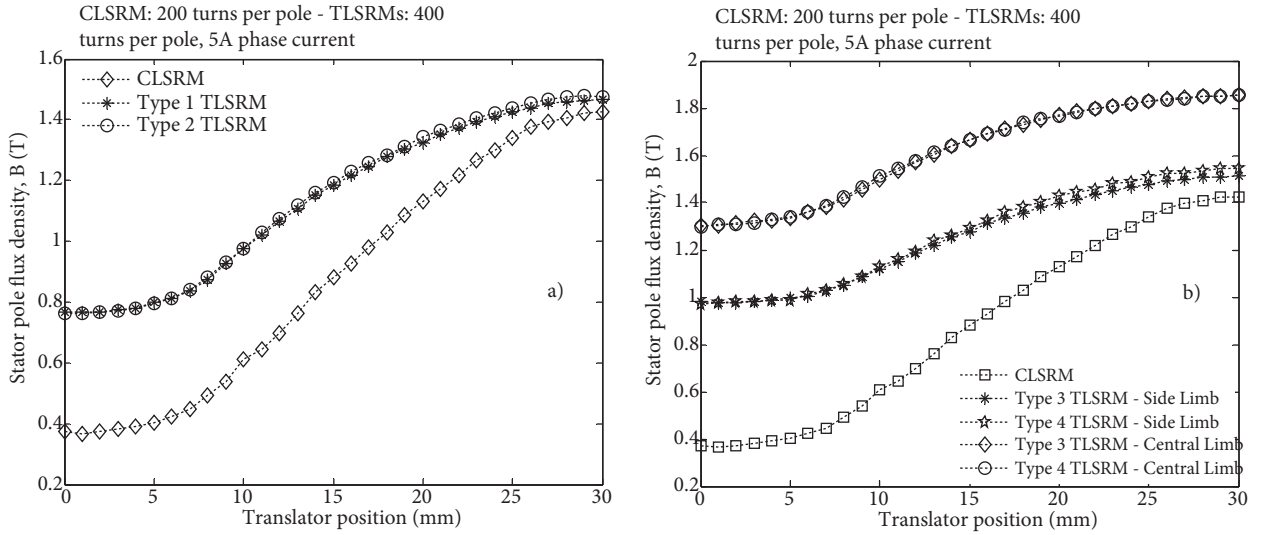

Figure 9. Stator pole flux density versus translator position for various types of LSRMs: a) CLSRM, type 1 and type 2 TLSRMs; b) CLSRM, type 3 and type 4 TLSRMs.

4.3. Equal propulsion force designs

The number of turns per pole of CLSRMs can be approximately calculated analytically for the maximum propulsion force, and there is also a similar propulsion force profile for equal current excitation of the CLSRM and TLSRMs. In addition, it is possible to calculate this value using the FEA results. The number of turns per pole of the TLSRMs is fixed at 400, as before, and the phase current is fixed at 5 A. Afterwards, the required number of turns per pole of the CLSRM is arrived at and can be calculated as 164. For this mmf, the propulsion force and mean flux density of the stator pole profiles of the motors are shown in Figures 10 and 11, respectively. CLSRMs generate a higher average propulsion force even when their stator pole flux density is lower than that of the TLSRMs.

Table 3. Comparison of LSRM structures for similar flux density.

Features	Type of LSRMs				
	CLSRM	Type 1 TLSRM	Type 2 TLSRM	Type 3 TLSRM	Type 4 TLSRM
Number of turns per pole	200	400	400	400	400
Phase current (A)	5	5	5	5	5
Stator volume (m^3)	4.62e-4	2.38e-4	2.38e-4	1.90e-4	1.90e-4
Translator volume (m^3)	3.53e-4	1.23e-4	0.77e-4	0.84e-5	0.38e-4
Winding volume (m^3)	1.86e-4	2.20e-4	2.20e-4	2.14e-4	2.14e-4
Active motor volume (m^3)	10.01e-4	5.81e-4	5.35e-4	4.88e-4	4.42e-4
Stator weight (kg)	4.14	2.13	2.13	1.70	1.70
Translator weight (kg)	3.16	1.10	0.69	0.76	0.34
Winding weight (kg)	1.68	1.96	1.96	1.92	1.92
Active motor weight (kg)	8.98	5.19	4.78	4.38	3.96
Average propulsion force (N)	49.72	27.18	27.79	28.23	28.26
Percentage force (%)	100	54.66	55.90	56.77	56.85
Percentage winding loss (%)	100	117	117	114	114
Force per active motor weight (Nm/kg)	5.54	5.24	5.81	6.44	7.14
Force density per copper weight (Nm/kg)	29.60	13.87	14.18	14.70	14.72

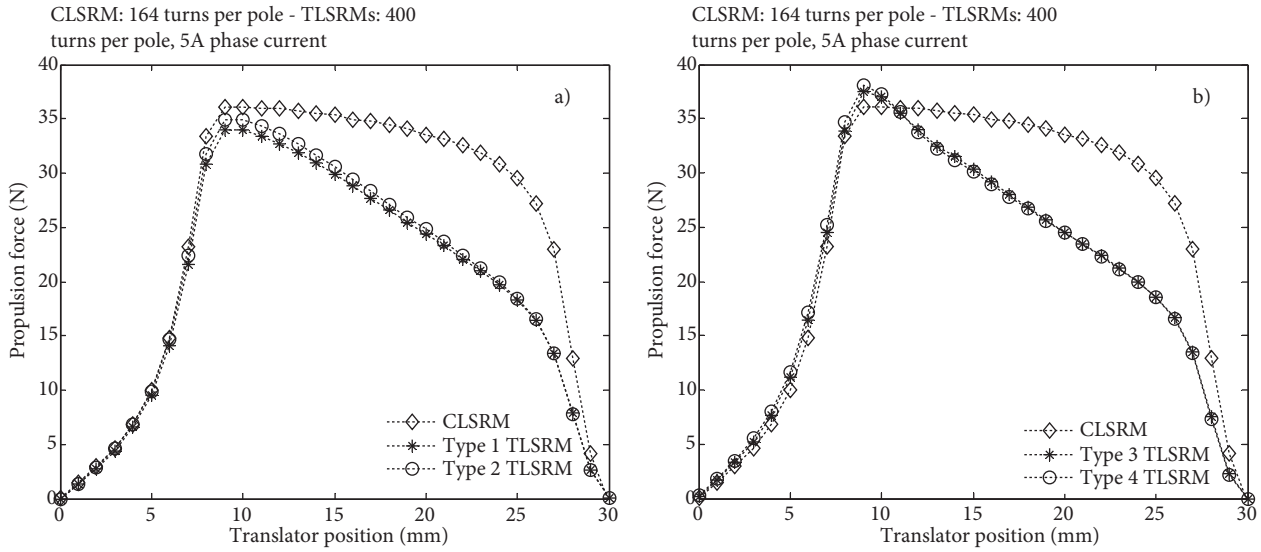

Figure 10. Propulsion forces versus translator position for various types of LSRMs with similar propulsion force profiles: a) CLSRM, type 1 and type 2 TLSRMs; b) CLSRM, type 3 and type 4 TLSRMs.

It is not possible to increase the number of turns per pole of the TLSRMs to reach propulsion force profiles similar to those of the CLSRM. Equal propulsion force can be obtained in both the CLSRM and TLSRMs by adjusting the number of turns to 86 and 200 turns per pole, respectively. Under such constraints, the propulsion force and stator pole mean flux density profiles of the motors are shown in Figures 12 and 13, respectively. Note the disparity in the number of turns per pole in the machines, with CLSRM showing absolute superiority in this respect.

The inductance profiles of the motors for the design parameters are shown in Figure 14, with the CLSRM having a consistently lower inductance than the TLSRMs by as much as 60% in an unaligned position and 30%

to 40% in an aligned position. Such decreased inductance has a major advantage in the dynamic control of the propulsion force by a flexible current control using the power converter, and in this regard the CLSRM performs better than the TLSRMs. The steady-state performance values and indices are given in Table 4.

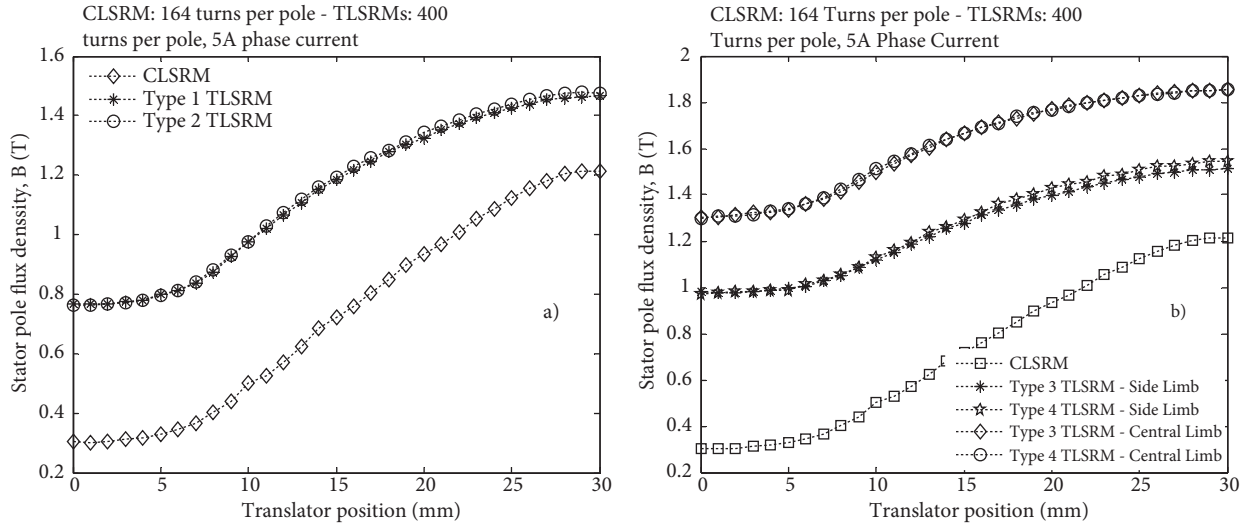

Figure 11. Flux Density versus translator position for various types of LSRMs: a) CLSRM, Type 1 and Type 2 TLSRMs b) CLSRM, Type 3 and Type 4 TLSRMs.

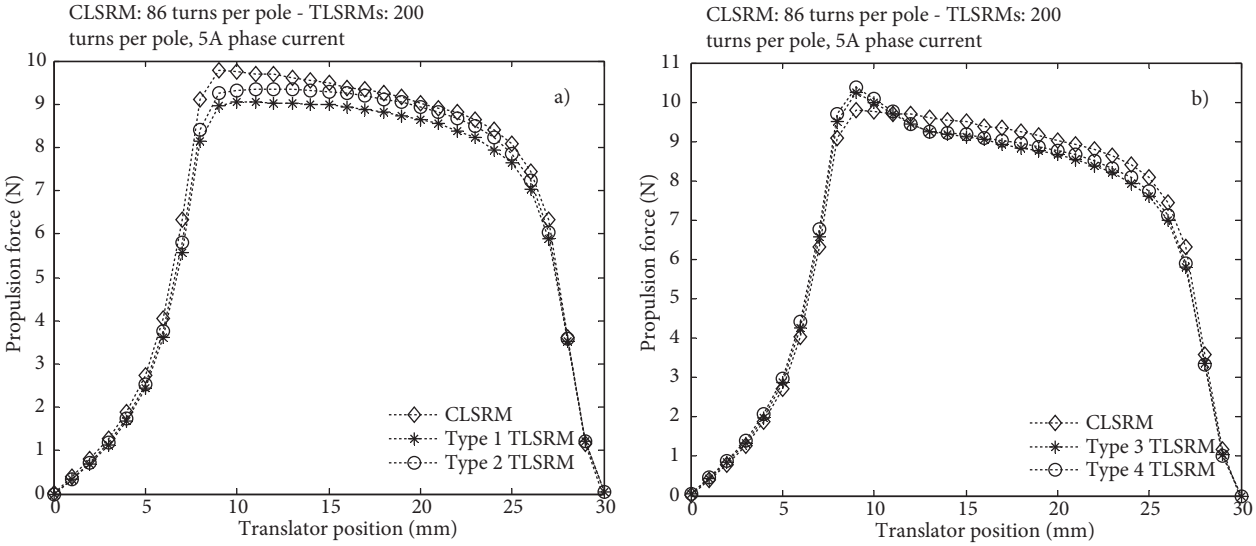

Figure 12. Propulsion forces versus translator position for various types of LSRMs with similar propulsion force profiles: a) CLSRM, type 1 and type 2 TLSRMs; b) CLSRM, type 3 and type 4 TLSRMs.

5. Constructional complexities

TLSRMs have many separate rotor and stator parts and require mechanical support structures to hold them in place, unlike the CLSRM stator and rotor bodies, which can be manufactured for a considerable stack length in one piece. The holding mechanical support structures for TLSRMs engender mechanical and assembly

complexities with an inevitable resulting increase in the cost of manufacture, and an exacerbation in vibration and noise is generated by bringing together disparate stator and rotor parts. These issues of complexity become much more formidable for larger systems in TLSRMs than in CLSRMs.

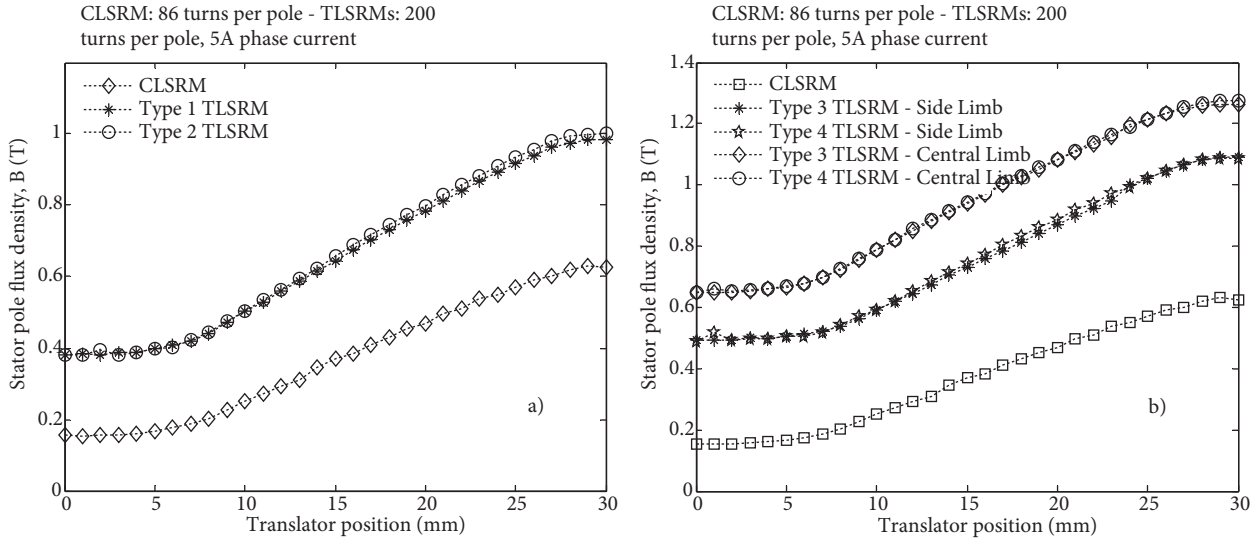

Figure 13. Stator pole flux density versus translator position for various types of LSRMs with similar force profiles: a) CLSRM, type 1 and type 2 TLSRMs; b) CLSRM, type 3 and type 4 TLSRMs.

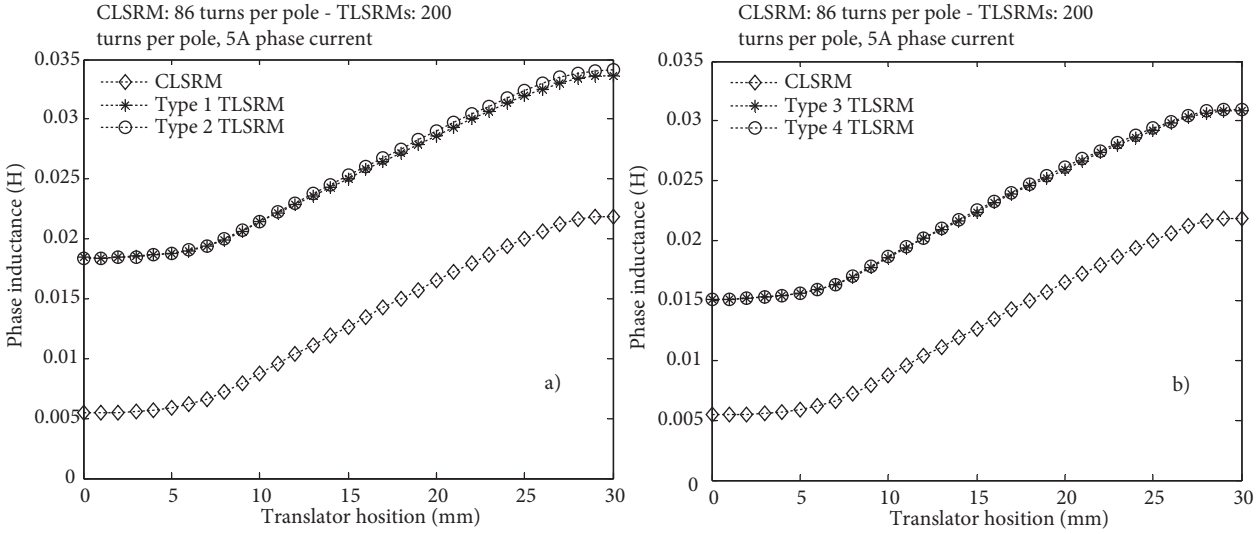

Figure 14. Phase inductance versus translator position for various types of LSRMs with similar force profiles: a) CLSRM, type 1 and type 2 TLSRMs; b) CLSRM, type 3 and type 4 TLSRMs.

6. Conclusions

A comprehensive comparative study of 4 types of TLSRM with a single-sided CLSRM has been made in this paper. Analytical and FEA approaches were used to predict the performance of the various designs of these machines. Some key observations from this research are:

Table 4. Comparison of LSRM structures for similar force profiles.

Features	Type of LSRM				
	CLSRM	Type 1 TLSRM	Type 2 TLSRM	Type 3 TLSRM	Type 4 TLSRM
Number of turns per pole	86	200	200	200	200
Phase current (A)	5	5	5	5	5
Stator volume (m^3)	4.62e-4	2.38e-4	2.38e-4	1.90e-4	1.90e-4
Translator volume (m^3)	3.53e-4	1.23e-4	0.77e-4	0.84e-5	0.38e-4
Winding volume (m^3)	0.80e-4	1.10e-4	1.10e-4	1.07e-4	1.07e-4
Active motor volume (m^3)	8.95e-4	4.71e-4	4.25e-4	3.81e-4	3.35e-4
Stator weight (kg)	4.14	2.13	2.13	1.70	1.70
Translator weight (kg)	3.16	1.10	0.69	0.76	0.34
Winding weight (kg)	0.72	0.98	0.98	0.96	0.96
Active motor weight (kg)	8.02	4.21	3.80	3.42	3.00
Average propulsion force (N)	8.97	8.43	8.71	8.74	8.85
Percentage force (%)	100	93.95	97.13	97.48	98.59
Percentage winding loss (%)	100	136	136	133	133
Force per active motor weight (Nm/kg)	1.12	2.00	2.29	2.55	2.95
Force density per copper weight (Nm/kg)	12.46	8.60	8.89	9.10	9.22

1. Based on linear operational characteristics of the machines, it has been proven that CLSRM has 6 times the propulsion force-generating capability of all the TLSRMs presented.

2. The high propulsion force-generating capability of the CLSRM is confirmed by the simulation for a design with an equal number of turns per pole in both machine structures.

3. The CLSRM fares well compared to TLSRMs in such performance indices as propulsion force per active weight and propulsion force per unit copper weight.

4. The complexity of construction in the CLSRM is much less severe than in all TLSRMs, leading to a cost-effective solution for linear motion applications.

Acknowledgment

N Üstkoyuncu thanks Kayseri ve Civarı Elektrik TAŞ for its financial support to him during his research at Virginia Polytechnic Institute and State University.

References

[1] Krishnan R. Switched Reluctance Motor Drives: Modeling, Simulation, Analysis, Design And Applications. New York, NY, USA: CRC Press, 2001.

[2] Bae HK, Lee BS, Vijayraghavan P, Krishnan R. A linear switched reluctance motor: Converter and control. IEEE T Ind Appl 2000; 36: 1351–1359.

[3] Lee BS, Bae HK, Vijayraghavan P, Krishnan R. Design of a linear switched reluctance machine. IEEE T Ind Appl 2000; 36: 1571–1580.

[4] Gan WC, Cheung NC, Qiu L. Position control of linear switched reluctance motors for high-precision applications. IEEE T Ind Appl 2003; 39: 1350–1362.

[5] Zhao SW, Cheung NC, Gan WC, Yang J, Pan JF. A self-tuning regulator for the high-precision position control of a linear switched reluctance motor. IEEE T Ind Electron 2007; 54: 2425–2434.

[6] Lim HS, Krishnan R. Ropeless elevator with linear switched reluctance motor drive actuation systems. IEEE T Ind Electron 2007; 54: 2209–2218.

[7] Lobo NS, Lim HS, Krishnan R. Comparison of linear switched reluctance machines for vertical propulsion application: analysis, design and experimental correlation. IEEE T Ind Appl 2008; 44: 1134–1142.

[8] Lim HS, Krishnan R, Lobo NS. Design and control of a linear propulsion system for an elevator using linear switched reluctance motors. IEEE T Ind Electron 2008; 55: 534–542.

[9] Baoming G, Almeida AT, Ferreira FJTE. Design of transverse flux linear switched reluctance motor. IEEE T Magn 2009; 45: 113–119.

[10] Amoros JG, Andrada P. Sensitivity analysis of geometrical parameters on a double-sided linear switched reluctance motor. IEEE T Ind Electron 2010; 57: 311–319.